Chapter 1

Offset continuation for reflection seismic data

In this chapter, I develop the theory of a regularization operator that is particularly suited for reflection seismic data. As discussed in Chapter **??**, an ideal regularization results from a data-space differential equation that we assume to be satisfied by the input data. Laplace's equation is appropriate for certain kinds of potential-field data, and the biharmonic equation applies to smooth elastic-type surfaces. A special differential equation is required to characterize the predictable features of seismic reflection data.

Fortunately, such an equation does exist. I introduce it in this chapter and study its theoretical properties. The equation describes the process of *offset continuation*, which is a transformation of common-offset seismic gathers from one constant offset to another (Bolondi et al., 1982). Bagaini et al. (1994) identified offset continuation (OC) with a whole family of prestack continuation operators, such as shot continuation (Schwab, 1993; Bagaini and Spagnolini, 1993), dip moveout as a continuation to zero offset, and three-dimensional azimuth moveout (Biondi and Chemingui, 1994a; Biondi et al., 1998).

The Earth subsurface is a three-dimensional object, while seismic reflection data from a multi-coverage acquisition belong to a five-dimensional space (time, 2-D offset, and 2-D midpoint coordinates). This fact alone is a clear indication of the additional connection that exists in the data space. The offset continuation equation expresses this connection in a concise mathematical form. Its theoretical analysis allows us to explain the data transformation between different offsets. A simple example is the diffraction point response shown in Figure 1.1 and analyzed theoretically later in this chapter.

As early as in 1982, Bolondi et al. came up with the idea of describing offset continuation and dip moveout (DMO) as a continuous process by means of a partial differential equation (Bolondi et al., 1982). However, their approximate differential operator, built on the results of Deregowski and Rocca's classic paper (Deregowski and Rocca, 1981), failed in the cases of steep reflector dips or large offsets. Hale (1983) writes:

> The differences between this algorithm [DMO by Fourier transform] and previously published finite-difference DMO algorithms are analogous to the differences between frequency-wavenumber (Stolt, 1978; Gazdag, 1978) and finite-difference (Claerbout, 1976) algorithms for migration. For example, just as finite-difference migration algorithms require approximations that break down at steep dips, finite-difference DMO algorithms are inaccurate for large offsets and steep dips, even for constant velocity.

Continuing this analogy, one can observe that both finite-difference and frequency-domain migration algorithms share a common origin: the wave equation. The new OC equation, presented in this chapter[1] and valid for all offsets and dips, plays a role analogous to that of the wave equation for offset continuation and dip moveout algorithms. A multitude of seismic migration algorithms emerged from the fundamental wave-propagation theory that is embedded in the wave equation. Likewise, the fundamentals of DMO algorithms can be traced to the OC differential equation.

In the first part of the chapter, I prove that the revised equation is, under certain assumptions, kinematically valid. This means that wavefronts of the offset continuation process correspond to the reflection wave traveltimes and correctly transform between different offsets. Moreover, the wave amplitudes are also propagated correctly according to the *true-amplitude* criterion (Black et al., 1993). The amplitude and phase preservation is additionally confirmed

[1]To my knowledge, the first derivation of the revised offset continuation equation was accomplished by Joseph Higginbotham of Texaco in 1989. Unfortunately, Higginbotham's derivation never appeared in the open literature.

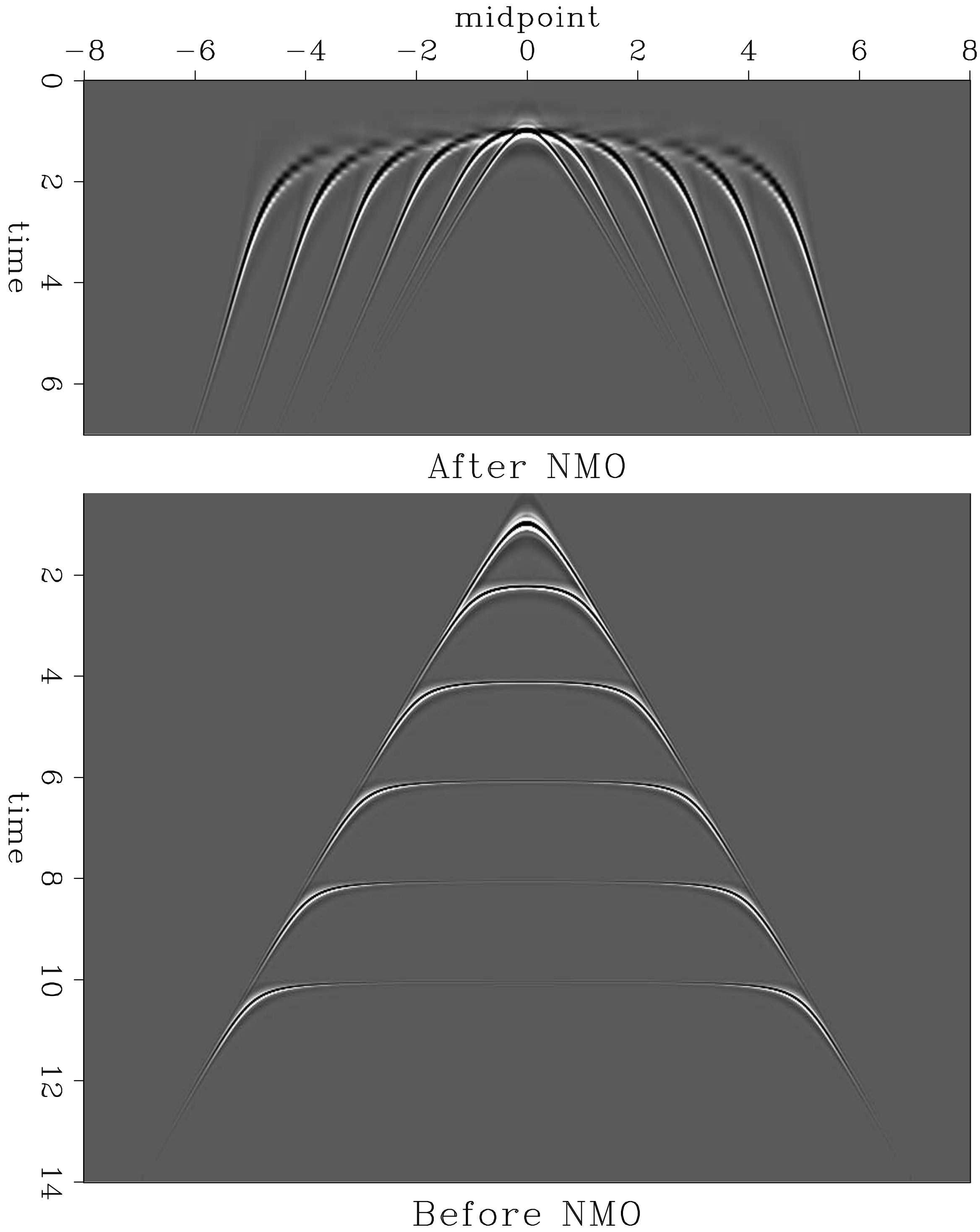

Figure 1.1: Common-offset sections of a diffraction point response (superimposed on the same plot). Top: after NMO. Bottom: before NMO. The offsets are 0, 1, 2, 3, 4, and 5 km. The offset continuation equation describes the data transformation between different offsets (see the left plot in Figure 1.5). ofcon-spik [ER]

by a direct theoretical test, where I represent the input common-offset data by the Kirchhoff modeling integral (Bleistein, 1984). The first two asymptotic orders of accuracy are satisfied when the offset continuation equation is applied to the Kirchhoff data.

In the second part of the chapter, I relate the offset continuation equation to different methods of dip moveout. Considering DMO as a continuation to zero offset, I show that DMO operators can be obtained by solving a special initial value (Cauchy-type) problem for the OC equation. Different known forms of DMO (Hale, 1991) appear as special cases of more general offset continuation operators.

INTRODUCING THE OFFSET CONTINUATION EQUATION

Most of the contents of this chapter refer to the following linear partial differential equation:

$$h\left(\frac{\partial^2 P}{\partial y^2} - \frac{\partial^2 P}{\partial h^2}\right) = t_n \, \frac{\partial^2 P}{\partial t_n \, \partial h} \; . \tag{1.1}$$

Equation (1.1) describes an *artificial* (non-physical) process of transforming reflection seismic data $P(y,h,t_n)$ in the offset-midpoint-time domain. In equation (1.1), h stands for the half-offset ($h = (r-s)/2$, where s and r are the source and the receiver coordinates), y is the midpoint ($y = (r+s)/2$), and t_n is the time coordinate after normal moveout correction is applied:

$$\left(t_n = \sqrt{t^2 - \frac{4\,h^2}{v^2}}\right) \; . \tag{1.2}$$

The velocity v is assumed to be known a priori. Equation (1.1) belongs to the class of linear hyperbolic equations, with the offset h acting as a time-like variable. It describes a wave-like propagation in the offset direction.

Proof of validity

A simplified version of the ray method technique (Červený et al., 1977; Babich, 1991) can allow us to prove the theoretical validity of equation (1.1) for all offsets and reflector dips by deriving two equations that describe separately wavefront (traveltime) and amplitude transformation. According to the formal ray theory, the leading term of the high-frequency asymptotics for a reflected wave recorded on a seismogram takes the form

$$P\,(y,h,t_n) \approx A_n(y,h)\,R_n\,(t_n-\tau_n(y,h))\ , \tag{1.3}$$

where A_n stands for the amplitude, R_n is the wavelet shape of the leading high-frequency term, and τ_n is the traveltime curve after normal moveout. Inserting (1.3) as a trial solution for (1.1), collecting terms that have the same asymptotic order (correspond to the same-order derivatives of the wavelet R_n), and neglecting low-order terms, we obtain a set of two first-order partial differential equations:

$$h\left[\left(\frac{\partial \tau_n}{\partial y}\right)^2-\left(\frac{\partial \tau_n}{\partial h}\right)^2\right]=-\,\tau_n\,\frac{\partial \tau_n}{\partial h}\ , \tag{1.4}$$

$$\left(\tau_n-2h\,\frac{\partial \tau_n}{\partial h}\right)\frac{\partial A_n}{\partial h}+2h\frac{\partial \tau_n}{\partial y}\frac{\partial A_n}{\partial y}+h\,A_n\left(\frac{\partial^2 \tau_n}{\partial y^2}-\frac{\partial^2 \tau_n}{\partial h^2}\right)=0\ . \tag{1.5}$$

Equation (1.4) describes the transformation of traveltime curve geometry in the OC process analogously to how the eikonal equation describes the front propagation in the classic wave theory. What appear to be wavefronts of the wave motion described by equation (1.1) are traveltime curves of reflected waves recorded on seismic sections. The law of amplitude transformation for high-frequency wave components related to those wavefronts is given by equation (1.5). In terms of the theory of partial differential equations, equation (1.4) is the characteristic equation for (1.1).

Proof of kinematic equivalence

In order to prove the validity of equation (1.4), it is convenient to transform it to the coordinates of the initial shot gathers: $s = y - h$, $r = y + h$, and $\tau = \sqrt{\tau_n^2 + \frac{4h^2}{v^2}}$. The transformed equation takes the form

$$\left(\tau^2 + \frac{(r-s)^2}{v^2}\right)\left(\frac{\partial \tau}{\partial r} - \frac{\partial \tau}{\partial s}\right) = 2\,(r-s)\,\tau\left(\frac{1}{v^2} - \frac{\partial \tau}{\partial r}\frac{\partial \tau}{\partial s}\right) \; . \tag{1.6}$$

Now the goal is to prove that any reflection traveltime function $\tau(r,s)$ in a constant velocity medium satisfies equation (1.6).

Let S and R be the source and the receiver locations, and O be a reflection point for that pair. Note that the incident ray SO and the reflected ray OR form a triangle with the basis on the offset SR ($l = |SR| = |r-s|$). Let α_1 be the angle of SO from the vertical axis, and α_2 be the analogous angle of RO (Figure 1.2). The law of sines gives us the following explicit relationships between the sides and the angles of the triangle SOR:

$$|SO| = |SR|\,\frac{\cos\alpha_1}{\sin(\alpha_2-\alpha_1)} \; , \tag{1.7}$$

$$|RO| = |SR|\,\frac{\cos\alpha_2}{\sin(\alpha_2-\alpha_1)} \; . \tag{1.8}$$

Hence, the total length of the reflected ray satisfies

$$v\tau = |SO| + |RO| = |SR|\,\frac{\cos\alpha_1 + \cos\alpha_2}{\sin(\alpha_2-\alpha_1)} = |r-s|\,\frac{\cos\alpha}{\sin\gamma} \; . \tag{1.9}$$

Here γ is the reflection angle ($\gamma = (\alpha_2 - \alpha_1)/2$), and α is the central ray angle ($\alpha = (\alpha_2 + \alpha_1)/2$), which coincides with the local dip angle of the reflector at the reflection point. Recalling the well-known relationships between the ray angles and the first-order traveltime derivatives

$$\frac{\partial \tau}{\partial s} = \frac{\sin\alpha_1}{v} \; , \tag{1.10}$$

$$\frac{\partial \tau}{\partial r} = \frac{\sin\alpha_2}{v} \; , \tag{1.11}$$

we can substitute (1.9), (1.10), and (1.11) into (1.6), which leads to the simple trigonometric equality

$$\cos^2\left(\frac{\alpha_1+\alpha_2}{2}\right)+\sin^2\left(\frac{\alpha_1-\alpha_2}{2}\right) = 1-\sin\alpha_1\sin\alpha_2\ . \tag{1.12}$$

It is now easy to show that equality (1.12) is true for any α_1 and α_2, since

$$\sin^2 a-\sin^2 b = \sin(a+b)\,\sin(a-b)\ .$$

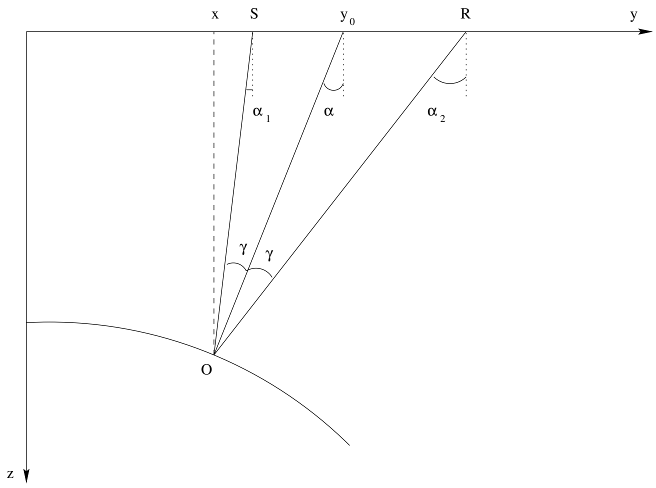

Figure 1.2: Reflection rays in a constant velocity medium (a scheme). ofcon-ocoray [NR]

Thus we have proved that equation (1.6), equivalent to (1.4), is valid in constant velocity media independently of the reflector geometry and the offset. This means that high-frequency asymptotic components of the waves, described by the OC equation, are located on the true reflection traveltime curves.

The theory of characteristics can provide other ways to prove the kinematic validity of equation (1.4), as described by Fomel (1994) and Goldin (1994).

Comparison with Bolondi's OC equation

Equation (1.1) and the previously published OC equation (Bolondi et al., 1982) differ only with respect to the single term $\frac{\partial^2 P}{\partial h^2}$. However, this difference is substantial.

From the offset continuation characteristic equation (1.4), we can conclude that the first-order traveltime derivative with respect to offset decreases with a decrease of the offset. At zero offset the derivative equals zero, as predicted by the principle of reciprocity (the reflection traveltime has to be an *even* function of offset). Neglecting $\frac{\partial \tau_n}{\partial h}$ in (1.4) leads to the characteristic equation

$$h \left(\frac{\partial \tau_n}{\partial y}\right)^2 = -\,\tau_n \frac{\partial \tau_n}{\partial h}\;, \tag{1.13}$$

which corresponds to the approximate OC equation of Bolondi et al. (1982). The approximate equation has the form

$$h \frac{\partial^2 P}{\partial y^2} = t_n \frac{\partial^2 P}{\partial t_n\, \partial h}\;. \tag{1.14}$$

Comparing (1.13) and (1.4), note that approximation (1.13) is valid only if

$$\left(\frac{\partial \tau_n}{\partial h}\right)^2 \ll \left(\frac{\partial \tau_n}{\partial y}\right)^2\;. \tag{1.15}$$

To find the geometric constraints implied by inequality (1.15), we can express the traveltime derivatives in geometric terms. As follows from expressions (1.10) and (1.11),

$$\frac{\partial \tau}{\partial x} = \frac{\partial \tau}{\partial r} + \frac{\partial \tau}{\partial s} = \frac{2 \sin\alpha \cos\gamma}{v}\;, \tag{1.16}$$

$$\frac{\partial \tau}{\partial h} = \frac{\partial \tau}{\partial r} - \frac{\partial \tau}{\partial s} = \frac{2 \cos\alpha \sin\gamma}{v}\;. \tag{1.17}$$

Expression (1.9) allows transforming equations (1.16) and (1.17) to the form

$$\tau_n \frac{\partial \tau_n}{\partial y} = \tau \frac{\partial \tau}{\partial y} = 4h \frac{\sin\alpha \cos\alpha \cot\gamma}{v^2}\;;\;; \tag{1.18}$$

$$\tau_n \frac{\partial \tau_n}{\partial h} = \tau \frac{\partial \tau}{\partial h} - \frac{4h}{v^2} = -4h \frac{\sin^2\alpha}{v^2}\;. \tag{1.19}$$

Without loss of generality, we can assume α to be positive. Consider a plane tangent to a true reflector at the reflection point (Figure 1.3). The traveltime of a wave, reflected from the plane, has the well-known explicit expression

$$\tau = \frac{2}{v}\sqrt{L^2 + h^2 \cos^2\alpha} \ , \tag{1.20}$$

where L is the length of the normal ray from the midpoint. As follows from combining (1.20) and (1.9),

$$\cos\alpha \cot\gamma = \frac{L}{h} \ . \tag{1.21}$$

We can then combine equalities (1.21), (1.18), and (1.19) to transform inequality (1.15) to the form

$$h \ll \frac{L}{\sin\alpha} = z \cot\alpha \ , \tag{1.22}$$

where z is the depth of the plane reflector under the midpoint. For example, for a dip of 45 degrees, equation (1.14) is satisfied only for offsets that are much smaller than the depth.

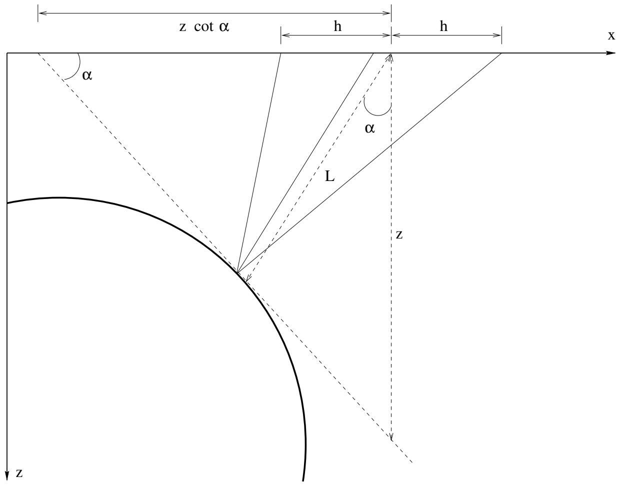

Figure 1.3: Reflection rays and tangent to the reflector in a constant velocity medium (a scheme). $\boxed{\text{ofcon-ocobol}}$ [NR]

Offset continuation geometry: time rays

To study the laws of traveltime curve transformation in the OC process, it is convenient to apply the method of characteristics (Courant, 1962) to the eikonal-type equation (1.4). The characteristics of equation (1.4) [*bi*-characteristics with respect to equation (1.1)] are the trajectories of the high-frequency energy propagation in the imaginary OC process. Following the formal analogy with seismic rays, I call those trajectories *time rays*, where the word *time* refers to the fact that the trajectories describe the traveltime transformation (Fomel, 1994). According to the theory of first-order partial differential equations, time rays are determined by a set of ordinary differential equations (characteristic equations) derived from equation (1.4) :

$$\begin{aligned} \frac{dy}{dt_n} = -\frac{2hY}{t_n H}\,,\ \frac{dY}{dt_n} = \frac{Y}{t_n}\,, \\ \frac{dh}{dt_n} = -\frac{1}{H} + \frac{2h}{t_n}\,,\ \frac{dH}{dt_n} = \frac{Y^2}{t_n H}\,, \end{aligned} \tag{1.23}$$

where Y corresponds to $\frac{\partial \tau_n}{\partial y}$ along a ray and H corresponds to $\frac{\partial \tau_n}{\partial h}$. In this notation, equation (1.4) takes the form

$$h\,(Y^2 - H^2) = -\,t_n H \tag{1.24}$$

and serves as an additional constraint for the definition of time rays. System (1.23) can be solved by standard mathematical methods (Tenenbaum and Pollard, 1985). Its general solution takes the parametric form, where the time variable t_n is the parameter changing along a time ray:

$$y(t_n) = C_1 - C_2\,t_n^2 \quad ; \quad h(t_n) = t_n\sqrt{C_2^2 t_n^2 + C_3}\,; \tag{1.25}$$

$$Y(t_n) = \frac{C_2\,t_n}{C_3} \quad ; \quad H(t_n) = \frac{h}{C_3\,t_n} \tag{1.26}$$

and C_1, C_2, and C_3 are independent coefficients, constant along each time ray. To determine the values of these coefficients, we can pose an initial-value (Cauchy) problem for the system of differential equations (1.23). The traveltime curve $\tau_n(y;h)$ for a given common offset h and the first partial derivative $\frac{\partial \tau_n}{\partial h}$ along the same constant offset section provide natural initial conditions for the Cauchy problem. A particular case of those conditions is the zero-offset traveltime curve. If the first partial derivative of traveltime with respect to offset is continuous, it vanishes at zero offset according to the reciprocity principle (traveltime must be an even function of the offset):

$$t_0\,(y_0) = \tau_n(y;0),\; \left.\frac{\partial \tau_n}{\partial h}\right|_{h=0} = 0\,. \tag{1.27}$$

Applying the initial-value conditions to the general solution (1.26) generates the following expressions for the ray invariants:

$$\begin{aligned} C_1 &= y + h\,\frac{Y}{H} = y_0 - \frac{t_0\,(y_0)}{t_0'\,(y_0)}\;;\; C_2 = \frac{h\,Y}{\tau_n^2\,H} = -\frac{1}{t_0\,(y_0)\,t_0'\,(y_0)}\;; \\ C_3 &= \frac{h}{\tau_n\,H} = -\frac{1}{\left(t_0'\,(y_0)\right)^2}\,, \end{aligned} \tag{1.28}$$

where $t_0'\,(y_0)$ denotes the derivative $\frac{d\,t_0}{d\,y_0}$. Finally, substituting (1.28) into (1.26), we obtain an explicit parametric form of the ray trajectories:

$$\left\{\begin{aligned} y_1\,(t_1) &= y + \frac{h\,Y}{t_n^2\,H}\left(t_n^2 - t_1^2\right) = y_0 + \frac{t_1^2 - t_0^2\,(y_0)}{t_0\,(y_0)\,t_0'\,(y_0)}\;; \\ h_1^2\,(t_1) &= \frac{h\,t_1^2}{t_n^3\,H}\left(t_n^2 + t_1^2\,\frac{h\,Y^2}{t_n\,H}\right) = t_1^2\,\frac{t_1^2 - t_0^2\,(y_0)}{\left(t_0\,(y_0)\,t_0'\,(y_0)\right)^2}\,. \end{aligned}\right. \tag{1.29}$$

Here y_1, h_1, and t_1 are the coordinates of the continued seismic section. The first of equations (1.29) indicates that the time ray projections to a common-offset section have a parabolic form. Time rays do not exist for $t_0'\,(y_0) = 0$ (a locally horizontal reflector) because in this case post-NMO offset continuation transform is not required.

The actual parameter that determines a particular time ray is the reflection point location. This important conclusion follows from the known parametric equations

$$\left\{\begin{aligned} t_0(x) &= t_v \sec\alpha = t_v(x)\sqrt{1 + u^2\left(t_v'(x)\right)^2}\,, \\ y_0(x) &= x + u t_v \tan\alpha = x + u^2\,t_v(x) t_v'(x)\,, \end{aligned}\right. \tag{1.30}$$

where x is the reflection point, u is half of the wave velocity ($u = v/2$), t_v is the vertical time (reflector depth divided by u), and α is the local reflector dip. Taking into account that the derivative of the zero-offset traveltime curve is

$$\frac{dt_0}{dy_0} = \frac{t_0'(x)}{y_0'(x)} = \frac{\sin\alpha}{u} = \frac{t_v'(x)}{\sqrt{1+u^2\left(t_v'(x)\right)^2}} \tag{1.31}$$

and substituting (1.30) into (1.29), we get

$$\left\{\begin{array}{rcl} y_1\,(t_1) & = & x + \dfrac{t_1^2 - t_v^2\,(x)}{t_v\,(x)\,t_v'\,(x)}\;; \\ \\ u^2 t^2\,(t_1) & = & t_1^2\,\dfrac{t_1^2 - t_v^2\,(x)}{\left(t_v\,(x)\,t_v'\,(x)\right)^2}\;, \end{array}\right. \tag{1.32}$$

where $t^2\,(t_1) = t_1^2 + h_1^2\,(t_1)\,/u^2$.

To visualize the concept of time rays, let us consider some simple analytic examples of its application to geometric analysis of the offset-continuation process.

The simplest and most important example is the case of a plane dipping reflector. Putting the origin of the y axis at the intersection of the reflector plane with the surface, we can express the reflection traveltime after NMO in the form

$$\tau_n(y,h) = p\sqrt{y^2 - h^2}\;, \tag{1.33}$$

where $p = 2\,\frac{\sin\alpha}{v}$, and α is the dip angle. The zero-offset traveltime in this case is a straight line:

$$t_0\,(y_0) = p\,y_0\;. \tag{1.34}$$

According to equations (1.29), the time rays in this case are defined by

$$y_1\,(t_1) = \frac{t_1^2}{p^2\,y_0}\;;\; h_1^2(t_1) = t_1^2\,\frac{t_1^2 - p^2\,y_0^2}{p^4\,y_0^2}\;;\; y_0 = \frac{y^2 - h^2}{y}\;. \tag{1.35}$$

The geometry of the OC transformation is shown in Figure 1.4.

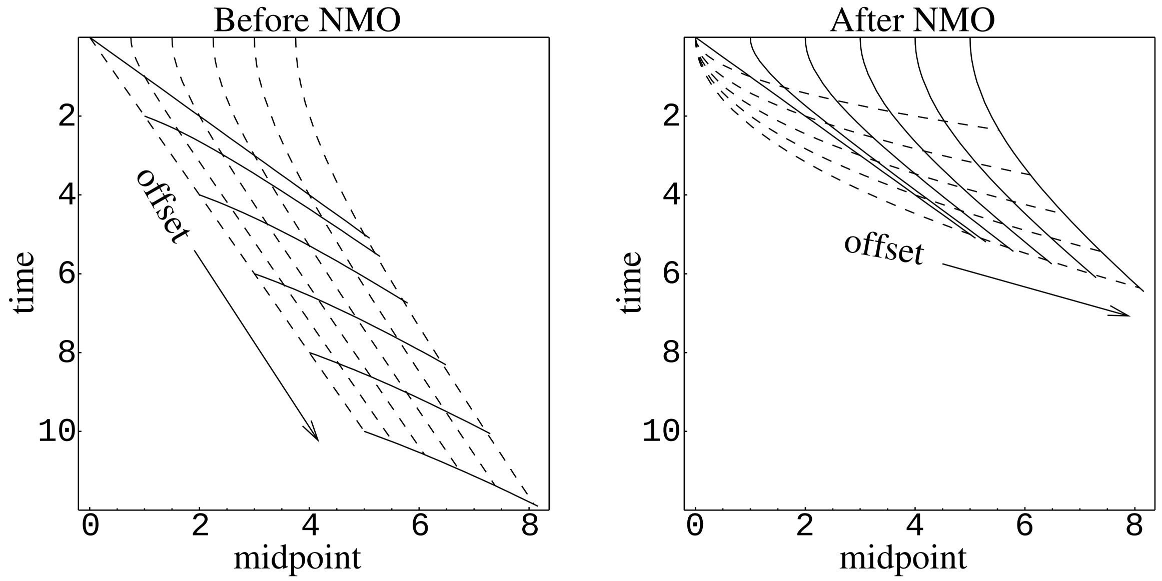

Figure 1.4: Transformation of the reflection traveltime curves in the OC process: the case of a plane dipping reflector. Left: Time coordinate before the NMO correction. Right: Time coordinate after NMO. The solid lines indicate traveltime curves at different common-offset sections; the dashed lines indicate time rays. ofcon-ocopln [NR]

The second example is the case of a point diffractor (the left side of Figure 1.5). Without loss of generality, the origin of the midpoint axis can be put above the diffraction point. In this case the zero-offset reflection traveltime curve has the well-known hyperbolic form

$$t_0\,(y_0) = \frac{\sqrt{z^2 + y_0^2}}{u}\;, \tag{1.36}$$

where z is the depth of the diffractor and $u = v/2$ is half of the wave velocity. Time rays are defined according to equations (1.29), as follows:

$$y_1\,(t_1) = \frac{u^2\,t_1^2 - z^2}{y_0}\;;\; u^2\,t^2\,(t_1) = u^2\,t_1^2 + h_1^2\,(t_1) = u^2\,t_1^2\,\frac{u^2\,t_1^2 - z^2}{y_0^2}\;. \tag{1.37}$$

The third example (the right side of Figure 1.5) is the curious case of a focusing elliptic reflector. Let y be the center of the ellipse and h be half the distance between the foci of

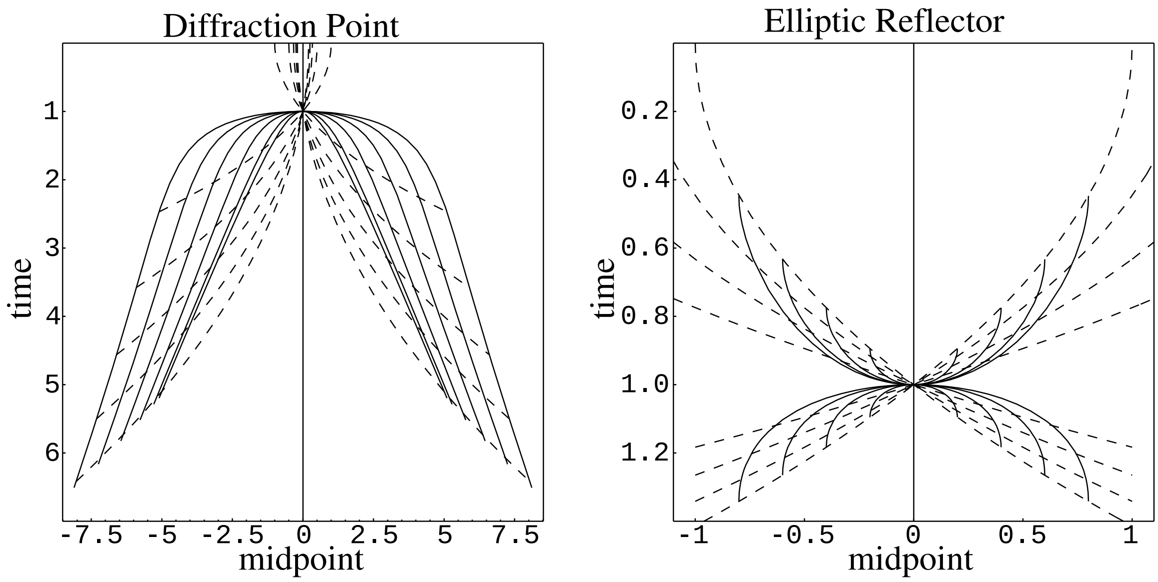

Figure 1.5: Transformation of the reflection traveltime curves in the OC process. Left: the case of a diffraction point. Right: the case of an elliptic reflector. Solid lines indicate traveltime curves at different common-offset sections, dashed lines indicate time rays. ofcon-ococrv [NR]

the ellipse. If both foci are on the surface, the zero-offset traveltime curve is defined by the so-called "DMO smile" (Deregowski and Rocca, 1981):

$$t_0\,(y_0) = \frac{t_n}{h}\,\sqrt{h^2-(y-y_0)^2}\;, \tag{1.38}$$

where $t_n = 2\,z/v$, and z is the small semi-axis of the ellipse. The time-ray equations are

$$y_1\,(t_1) = y + \frac{h^2}{y-y_0}\,\frac{t_1^2-t_n^2}{t_n^2}\;;\; h_1^2(t_1) = h^2\,\frac{t_1^2}{t_n^2}\left(1+\frac{h^2}{(y-y_0)^2}\,\frac{t_1^2-t_n^2}{t_n^2}\right)\;. \tag{1.39}$$

When y_1 coincides with y, and h_1 coincides with h, the source and the receiver are in the foci of the elliptic reflector, and the traveltime curve degenerates to a point $t_1 = t_n$. This remarkable fact is the actual basis of the geometric theory of dip moveout (Deregowski and Rocca, 1981).

Proof of amplitude equivalence

This section discusses the connection between the laws of traveltime transformation and the laws of the corresponding amplitude transformation. The change of the wave amplitudes in the OC process is described by the first-order partial differential transport equation (1.5). We can find the general solution of this equation by applying the method of characteristics. The solution takes the explicit integral form

$$A_n(t_n) = A_0(t_0)\exp\left(\int_{t_o}^{t_n}\left[h\left(\frac{\partial^2\tau_n}{\partial y^2}-\frac{\partial^2\tau_n}{\partial h^2}\right)\left(\tau_n\frac{\partial\tau_n}{\partial h}\right)^{-1}\right]d\tau_n\right). \tag{1.40}$$

The integral in equation (1.40) is defined on a curved time ray, and $A_n(t_n)$ stands for the amplitude transported along this ray. In the case of a plane dipping reflector, the ray amplitude can be immediately evaluated by substituting the explicit traveltime and time ray equations from the preceding section into (1.40). The amplitude expression in this case takes the simple form

$$A_n(t_n) = A_0(t_0)\exp\left(-\int_{t_o}^{t_n}\frac{d\tau_n}{\tau_n}\right) = A_0(t_0)\,\frac{t_0}{t_n}\,. \tag{1.41}$$

In order to consider the more general case of a curvilinear reflector, we need to take into account the connection between the traveltime derivatives in (1.40) and the geometry of the reflector. As follows directly from the trigonometry of the incident and reflected rays triangle (Figure 1.2),

$$h = \frac{r-s}{2} = D\,\frac{\cos\alpha\,\sin\gamma\,\cos\gamma}{\cos^2\alpha-\sin^2\gamma}\,, \tag{1.42}$$

$$y = \frac{r+s}{2} = x + D\,\frac{\cos^2\alpha\,\sin\alpha}{\cos^2\alpha-\sin^2\gamma}\,, \tag{1.43}$$

$$y_0 = x + D\,\sin\alpha\,, \tag{1.44}$$

where D is the length of the normal ray. Let $\tau_0 = 2\,D/v$ be the zero-offset reflection traveltime. Combining equations (1.42) and (1.44) with (1.9), we can get the following relationship:

$$a = \frac{\tau_n}{\tau_0} = \frac{\cos\alpha\,\cos\gamma}{\left(\cos^2\alpha - \sin^2\gamma\right)^{1/2}} = \left(1 + \frac{\sin^2\alpha\,\sin^2\gamma}{\cos^2\alpha - \sin^2\gamma}\right)^{1/2} = \frac{h}{\sqrt{h^2 - (y-y_0)^2}}\;, \tag{1.45}$$

which describes the "DMO smile" (1.38) found by Deregowski and Rocca (1981) in geometric terms. Equation (1.45) allows a convenient change of variables in (1.40). Let the reflection angle γ be a parameter monotonically increasing along a time ray. In this case, each time ray is uniquely determined by the position of the reflection point, which in turn is defined by the values of D and α. According to this change of variables, we can differentiate (1.45) along a time ray to get

$$\frac{d\tau_n}{\tau_n} = -\frac{\sin^2\alpha}{2\,\cos^2\gamma\,\left(\cos^2\gamma - \sin^2\alpha\right)}\,d\left(\cos^2\gamma\right)\;. \tag{1.46}$$

Note also that the quantity $h\left(\tau_n\,\frac{\partial\tau_n}{\partial h}\right)^{-1}$ in equation (1.40) coincides exactly with the time ray invariant C_3 found in equation (1.28). Therefore its value is constant along each time ray and equals

$$h\left(\tau_n\,\frac{\partial\tau_n}{\partial h}\right)^{-1} = -\frac{v^2}{4\,\sin^2\alpha}\;. \tag{1.47}$$

Finally, as shown in Appendix A,

$$\tau_n\left(\frac{\partial^2\tau_n}{\partial y^2} - \frac{\partial^2\tau_n}{\partial h^2}\right) = 4\,\frac{\cos^2\gamma}{v^2}\left(\frac{\sin^2\alpha + DK}{\cos^2\gamma + DK}\right)\;, \tag{1.48}$$

where K is the reflector curvature at the reflection point. Substituting (1.46), (1.47), and (1.48) into (1.40) transforms the integral to the form

$$\int_{t_o}^{t_n}\left[h\left(\frac{\partial^2\tau_n}{\partial y^2} - \frac{\partial^2\tau_n}{\partial h^2}\right)\left(\tau_n\,\frac{\partial\tau_n}{\partial h}\right)^{-1}\right]d\tau_n =$$

$$= -\frac{1}{2}\int_{\cos^2\gamma_0}^{\cos^2\gamma}\left(\frac{1}{\cos^2\gamma' - \sin^2\alpha} - \frac{1}{\cos^2\gamma' + DK}\right) d\left(\cos^2\gamma'\right) \tag{1.49}$$

which we can evaluate analytically. The final formula for the amplitude transformation takes the form

$$\begin{aligned} A_n &= A_0\,\frac{\sqrt{\cos^2\gamma - \sin^2\alpha}}{\sqrt{\cos^2\gamma_0 - \sin^2\alpha}}\left(\frac{\cos^2\gamma_0 + DK}{\cos^2\gamma + DK}\right)^{1/2} = \\ &= A_0\,\frac{\tau_0\,\cos\gamma}{\tau_n\,\cos\gamma_0}\left(\frac{\cos^2\gamma_0 + DK}{\cos^2\gamma + DK}\right)^{1/2} . \end{aligned} \tag{1.50}$$

In case of a plane reflector, the curvature K is zero, and (1.50) coincides with (1.41). Equation (1.50) can be rewritten as

$$A_n = \frac{c\,\cos\gamma}{\tau_n\,\sqrt{\cos^2\gamma + DK}} , \tag{1.51}$$

where c is constant along each time ray (it may vary with the reflection point location on the reflector but not with the offset). We should compare equation (1.51) with the known expression for the reflection wave amplitude of the leading ray series term in 2.5-D media:

$$A = \frac{C_R(\gamma)\Psi}{G} , \tag{1.52}$$

where C_R stands for the angle-dependent reflection coefficient, G is the geometric spreading

$$G = v\tau\,\frac{\sqrt{\cos^2\gamma + DK}}{\cos\gamma} , \tag{1.53}$$

and Ψ includes other possible factors (such as the source directivity) that we can either correct or neglect in the preliminary processing. It is evident that the curvature dependence of the amplitude transformation (1.51) coincides completely with the true geometric spreading factor (1.53) and that the angle dependence of the reflection coefficient is not provided by the offset continuation process. If the wavelet shape of the reflected wave on seismic sections [R_n in equation (1.3)] is described by the delta function, then, as follows from the known properties of this function,

$$A\,\delta\,(t-\tau(y,h)) = \left|\frac{dt_n}{dt}\right| A\,\delta\,(t_n-\tau_n(y,h)) = \frac{t}{t_n}\,A\,\delta\,(t_n-\tau_n(y,h))\;, \tag{1.54}$$

which leads to the equality

$$A_n = A\,\frac{t}{t_n}\;. \tag{1.55}$$

Combining equation (1.55) with equations (1.52) and (1.51) allows us to evaluate the amplitude after continuation from some initial offset h_0 to another offset h_1, as follows:

$$A_1 = \frac{C_R(\gamma_0)\Psi_0}{G_1}\;. \tag{1.56}$$

According to equation (1.56), the OC process described by equation (1.1) is amplitude-preserving in the sense that corresponds to Born DMO (Liner, 1991; Bleistein, 1990). This means that the geometric spreading factor from the initial amplitudes is transformed to the true geometric spreading on the continued section, while the reflection coefficient stays the same. This remarkable dynamic property allows AVO (amplitude versus offset) analysis to be performed by a dynamic comparison between true constant-offset sections and the sections transformed by OC from different offsets. With a simple trick, the offset coordinate is transferred to the reflection angles for the AVO analysis. As follows from (1.45) and (1.9),

$$\frac{\tau_n^2}{\tau\,\tau_0} = \cos\gamma\;. \tag{1.57}$$

If we include the $\frac{t_n^2}{t\,t_0}$ factor in the DMO operator (continuation to zero offset) and divide the result by the DMO section obtained without this factor, the resultant amplitude of the reflected events will be directly proportional to $\cos\gamma$, where the reflection angle γ corresponds to the initial offset. Of course, this conclusion is rigorously valid for constant-velocity 2.5-D media only.

Black et al. (1993) suggest a definition of true-amplitude DMO different from that of Born DMO. The difference consists of two important components:

1. *True-amplitude DMO addresses preserving the peak amplitude of the image wavelet instead of preserving its spectral density.* In the terms of this chapter, the peak amplitude corresponds to the pre-NMO amplitude A from formula (1.52) instead of corresponding to the spectral density amplitude A_n. A simple correction factor $\frac{t}{t_n}$ would help us take the difference between the two amplitudes into account. Multiplication by $\frac{t}{t_n}$ can be easily done at the NMO stage.

2. *Seismic sections are multiplied by time to correct for the geometric spreading factor prior to DMO (or, in our case, offset continuation) processing.*

As follows from (1.53), multiplication by t is a valid geometric spreading correction for plane reflectors only. It is the amplitude-preserving offset continuation based on the OC equation (1.1) that is able to correct for the curvature-dependent factor in the amplitude. To take into account the second aspect of Black's definition, we can consider the modified field $\hat{P}$ such that

$$\hat{P}\,(y,h,t_n) = t\;P\,(y,h,t_n)\;. \tag{1.58}$$

Substituting (1.58) into the OC equation (1.1) transforms the latter to the form

$$h\,\left(\frac{\partial^2 \hat{P}}{\partial y^2} - \frac{\partial^2 \hat{P}}{\partial h^2}\right) = t_n\,\frac{\partial^2 \hat{P}}{\partial t_n\,\partial h} - \frac{\partial \hat{P}}{\partial h}\;. \tag{1.59}$$

Equations (1.59) and (1.1) differ only with respect to the first-order damping term $\frac{\partial \hat{P}}{\partial h}$. This term affects the amplitude behavior but not the traveltimes, since the eikonal-type equation (1.4) depends on the second-order terms only. Offset continuation operators based on (1.59) conform to Black's definition of true-amplitude processing.

CONFIRMATION OF OFFSET CONTINUATION ON KIRCHHOFF DATA

Another confirmation of the kinematic and amplitude validity of the offset continuation equation follows from applying the equation to the Kirchhoff modeling approximation.

The Kirchhoff modeling approximation

In this subsection, I discuss the Kirchhoff approximate integral representation of the upward propagating response to a single reflector with separated source and receiver points. I then show how the amplitude of this integrand is related to the zero-offset amplitude at the source receiver point on the ray that makes equal angles at the scattering point with the rays from the separated source and receiver. The Kirchhoff integral representation (Haddon and Buchen, 1981; Bleistein, 1984) describes the wavefield scattered from a single reflector. This representation is applicable in situations where the high-frequency assumption is valid (the wavelength is smaller than the characteristic dimensions of the model) and corresponds in accuracy to the WKBJ approximation for reflected waves. The general form of the Kirchhoff modeling integral is

$$U_S(r,s,\omega) = \int_\Sigma R(x;r,s)\,\frac{\partial}{\partial n}\,[U_I(s,x,\omega)\,G(x,r,\omega)]\,d\Sigma\;, \tag{1.60}$$

where s and r stand for the source and the receiver locations; x denotes a point on the reflector surface Σ; R is the reflection coefficient at Σ; n is the upward normal to the reflector at the point x; and U_I and G are the incident wavefield and Green's function, respectively represented by their WKBJ approximation,

$$U_I(s,x,\omega) = F(\omega)\,A_s(s,x)\,e^{i\omega\tau_s(s,x)}\;, \tag{1.61}$$

$$G(x,r,\omega) = A_r(x,r)\,e^{i\omega\tau_r(x,r)}\;. \tag{1.62}$$

In this equation, $\tau_s(s,x)$ and $A_s(s,x)$ are the traveltime and the amplitude of the wave propagating from s to x; $\tau_r(x,r)$ and $A_r(x,r)$ are the corresponding quantities for the wave propagating from x to r; $F(\omega)$ is the spectrum of the input signal, assumed to be the transform of a band-limited impulsive source. In the time domain, the Kirchhoff modeling integral transforms to

$$u_S(r,s,t) = \int_\Sigma R(x;r,s)\,\frac{\partial}{\partial n}\left[A_s(s,x)\,A_r(x,r)\,f\left(t-\tau_s(s,x)-\tau_r(x,r)\right)\right]dx\;, \tag{1.63}$$

with f denoting the inverse temporal transform of F. The reflection traveltime τ_{sr} corresponds physically to the diffraction from a point diffractor located at the point x on the surface Σ, and the amplitudes A_s and A_r are point diffractor amplitudes.

The main goal of this section is to test the compliance of representation (1.63) with the offset continuation differential equation. The OC equation contains the derivatives of the wavefield with respect to the parameters of observation (s,r, and t). According to the rules of classic calculus, these derivatives can be taken under the sign of integration in formula (1.63). Furthermore, since we do not assume that the true-amplitude OC operator affects the reflection coefficient R, the offset-dependence of this coefficient is outside the scope of consideration. Therefore, the only term to be considered as a trial solution to the OC equation is the kernel of the Kirchhoff integral, which is contained in the square brackets in equations (1.60) and (1.63) and has the form

$$k(s,r,x,t) = A_{sr}(s,r,x)\, f\left(t - \tau_{sr}(s,r,x)\right) \;, \tag{1.64}$$

where

$$\begin{aligned} \tau_{sr}(s,r,x) &= \tau_s(s,x) + \tau_r(x,r)\,, & (1.65)\\ A_{sr}(s,r,x) &= A_s(s,x)\,A_r(x,r)\,. & (1.66) \end{aligned}$$

In a 3-D medium with a constant velocity v, the traveltimes and amplitudes have the simple explicit expressions

$$\tau_s(s,x) = \frac{\rho_s(s,x)}{v} \quad , \quad A_s(s,x) = \frac{1}{4\pi\;\rho_s(s,x)}\;, \tag{1.67}$$

$$\tau_r(x,r) = \frac{\rho_r(x,r)}{v} \quad , \quad A_r(x,r) = \frac{1}{4\pi\;\rho_r(x,r)}\;, \tag{1.68}$$

where ρ_s and ρ_r are the lengths of the incident and reflected rays, respectively (Figure 1.6). If the reflector surface Σ is explicitly defined by some function $z = z(x)$, then

$$\rho_s(s,x) = \sqrt{(x-s)^2 + z^2(x)}\,,\;\; \rho_r(x,r) = \sqrt{(r-x)^2 + z^2(x)}\,. \tag{1.69}$$

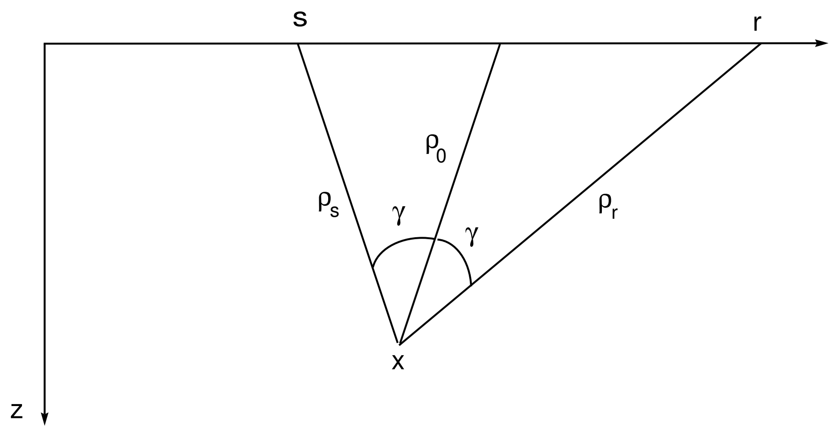

Figure 1.6: Geometry of diffraction in a constant-velocity medium: view in the reflection plane. ofcon-cwpgen [NR]

I then introduce a particular zero-offset amplitude, namely the amplitude along the zero offset ray that bisects the angle between the incident and reflected ray in this plane, as shown in Figure 1.6. Let us denote the square of this amplitude by A_0. That is,

$$A_0 = \frac{1}{(4\pi\rho_0)^2}\;. \tag{1.70}$$

As follows from equations (1.66) and (1.67-1.68), the amplitude transformation in DMO (continuation to zero offset) is characterized by the dimensionless ratio

$$\frac{A_{sr}}{A_0} = \frac{\rho_0^2}{\rho_s\,\rho_r}\;, \tag{1.71}$$

where ρ_0 is the length of the zero-offset ray (Figure 1.6).

As follows from the law of cosines,

$$\sqrt{\rho_s^2+\rho_0^2-2\,\rho_s\,\rho_0\,\cos\gamma}\;+\;\sqrt{\rho_r^2+\rho_0^2-2\,\rho_r\,\rho_0\,\cos\gamma} =$$
$$= \sqrt{\rho_s^2+\rho_r^2-2\,\rho_s\,\rho_r\,\cos 2\gamma}\;, \tag{1.72}$$

where γ is the reflection angle, as shown in the figure. After straightforward algebraic transformations of equation (1.72), we arrive at the explicit relationship between the ray lengths:

$$\frac{(\rho_s + \rho_r)\,\rho_0}{2\,\rho_s\,\rho_r} = \cos\gamma\;. \tag{1.73}$$

Substituting (1.73) into (1.71) yields

$$\frac{A_{sr}}{A_0} = \frac{\tau_0}{\tau_{sr}}\cos\gamma\;, \tag{1.74}$$

where τ_0 is the zero-offset two-way traveltime ($\tau_0 = 2\,\rho_0/v$).

What we have done is rewrite the finite-offset amplitude in the Kirchhoff integral in terms of a particular zero-offset amplitude. That zero-offset amplitude would arise as the geometric spreading effect if there were a reflector whose dip was such that the finite-offset pair would be specular at the scattering point. Of course, the zero-offset ray would also be specular in this case.

Kirchhoff model and the offset continuation equation

Equation (1.1) describes the process of seismogram transformation in the time-midpoint-offset domain. In order to obtain the high-frequency asymptotics of the equation's solution by standard methods, we can introduce a trial asymptotic solution of the form (1.3).

If we then rewrite the eikonal equation (1.4) in the time-source-receiver coordinate system as (1.6), we can easily[2] verify that the explicit expression for the phase of the Kirchhoff integral kernel (1.65) satisfies the eikonal equation for any scattering point x. Here, τ_{sr} is related to τ_n as t is related to t_n in equation (1.1).

The general solution of the amplitude equation (1.5) has the form

$$A_n = A_0\,\frac{\tau_0\cos\gamma}{\tau_n}\left(\frac{1+\rho_0\,K}{\cos^2\gamma+\rho_0\,K}\right)^{1/2}\;, \tag{1.75}$$

[2]using Mathematica

which is a particular form of the previously derived equation (1.50) for continuation from zero offset. Since the kernel (1.64) of the Kirchhoff integral (1.63) corresponds kinematically to the reflection from a point diffractor, we can obtain the solution of the amplitude equation for this case by formally setting the curvature K to infinity (setting the radius of curvature to zero). The infinite curvature transforms formula (1.75) to the relationship

$$\frac{A_n}{A_0} = \frac{\tau_0}{\tau_n} \cos\gamma \; . \tag{1.76}$$

Again, we exploit the assumption that the signal f has the form of the delta function. In this case, the amplitudes before and after the NMO correction are connected according to the known properties of the delta function, as follows:

$$A_{sr}\,\delta\left(t-\tau_{sr}(s,r,x)\right) = \left|\frac{\partial t_n}{\partial t}\right|_{t=\tau_{sr}} A_{sr}\,\delta\left(t_n-\tau_n(s,r,x)\right) = A_n\,\delta\left(t_n-\tau_n(s,r,x)\right) \; , \tag{1.77}$$

with

$$A_n = \frac{\tau_{sr}}{\tau_n} A_{sr} \; . \tag{1.78}$$

Combining equations (1.78) and (1.76) yields

$$\frac{A_{sr}}{A_0} = \frac{\tau_0}{\tau_{sr}} \cos\gamma \; , \tag{1.79}$$

which coincides exactly with the previously found equation (1.74).

It is apparent that the OC differential equation (1.1) and the Kirchhoff representation have the same effect on reflection data because the amplitude and phase of the former match those of the latter. Thus, we see that the amplitude and phase of the Kirchhoff representation for arbitrary offset correspond to the point diffractor WKBJ solution of the offset-continuation differential equation. Hence, the Kirchhoff approximation is a solution of the OC differential equation when we hold the reflection coefficient constant. This means that the solution of the OC differential equation has all the features of amplitude preservation, as does the Kirchhoff representation, including geometrical spreading, curvature effects, and phase shift effects. Furthermore, in the Kirchhoff representation and the solution of the OC partial differential equation by WKBJ, we have not used the 2.5-D assumption. Therefore the preservation of amplitude is not restricted to cylindrical surfaces as it is in Bleistein's and Cohen's (1995) true-amplitude proof for DMO.

THE CAUCHY PROBLEM AND THE INTEGRAL OPERATOR

Equation (1.1) describes a continuous process of reflected wavefield continuation in the time-offset-midpoint domain. In order to find an integral-type operator that performs the one-step offset continuation, I consider the following initial-value (Cauchy) problem for equation (1.1):

Given a post-NMO constant-offset section at half-offset h_1

$$P(t_n,h,y)|_{h=h_1} = P_1^{(0)}(t_n,y) \tag{1.80}$$

and its first-order derivative with respect to offset

$$\left.\frac{\partial P(t_n,h,y)}{\partial h}\right|_{h=h_1} = P_1^{(1)}(t_n,y)\,, \tag{1.81}$$

find the corresponding section $P^{(0)}(t_n,y)$ at offset h.

Equation (1.1) belongs to the hyperbolic type, with the offset coordinate h being a "time-like" variable and the midpoint coordinate y and the time t_n being "space-like" variables. The last condition (1.81) is required for the initial value problem to be well-posed (Courant, 1962). From a physical point of view, its role is to separate the two different wave-like processes embedded in equation (1.1), which are analogous to inward and outward wave propagation. We will associate the first process with continuation to a larger offset and the second one with continuation to a smaller offset. Though the offset derivatives of data are not measured in practice, they can be estimated from the data at neighboring offsets by a finite-difference approximation. Selecting a propagation branch explicitly, for example by considering the high-frequency asymptotics of the continuation operators, can allow us to eliminate the need for condition (1.81). In this section, I discuss the exact integral solution of the OC equation and analyze its asymptotics.

The integral solution of problem (1.80-1.81) for equation (1.1) is obtained in Appendix B with the help of the classic methods of mathematical physics. It takes the explicit form

$$\begin{aligned} P(t_n,h,y) &= \int\!\!\int P_1^{(0)}(t_1,y_1)\,G_0(t_1,h_1,y_1;t_n,h,y)\,dt_1\,dy_1 \\ &+ \int\!\!\int P_1^{(1)}(t_1,y_1)\,G_1(t_1,h_1,y_1;t_n,h,y)\,dt_1\,dy_1\;, \end{aligned} \tag{1.82}$$

where the Green's functions G_0 and G_1 are expressed as

$$G_0(t_1,h_1,y_1;t_n,h,y) = \mathrm{sign}(h-h_1)\,\frac{H(t_n)}{\pi}\,\frac{\partial}{\partial t_n}\left\{\frac{H(\Theta)}{\sqrt{\Theta}}\right\}, \tag{1.83}$$

$$G_1(t_1,h_1,y_1;t_n,h,y) = \mathrm{sign}(h-h_1)\,\frac{H(t_n)}{\pi}\,h\,\frac{t_n}{t_1^2}\left\{\frac{H(\Theta)}{\sqrt{\Theta}}\right\}, \tag{1.84}$$

and the parameter Θ is

$$\Theta(t_1,h_1,y_1;t_n,h,y) = \left(h_1^2/t_1^2 - h^2/t_n^2\right)\left(t_1^2 - t_n^2\right) - (y_1-y)^2\;. \tag{1.85}$$

H stands for the Heavyside step-function.

From equations (1.83) and (1.84) one can see that the impulse response of the offset continuation operator is discontinuous in the time-offset-midpoint space on a surface defined by the equality

$$\Theta(t_1,h_1,y_1;t_n,h,y) = 0\,, \tag{1.86}$$

which describes the "wavefronts" of the offset continuation process. In terms of the theory of characteristics (Courant, 1962), the surface $\Theta = 0$ corresponds to the characteristic conoid formed by the bi-characteristics of equation (1.1) – time rays emerging from the point $\{t_n,h,y\} = \{t_1,h_1,y_1\}$. The common-offset slices of the characteristic conoid are shown in the left plot of Figure 1.7.

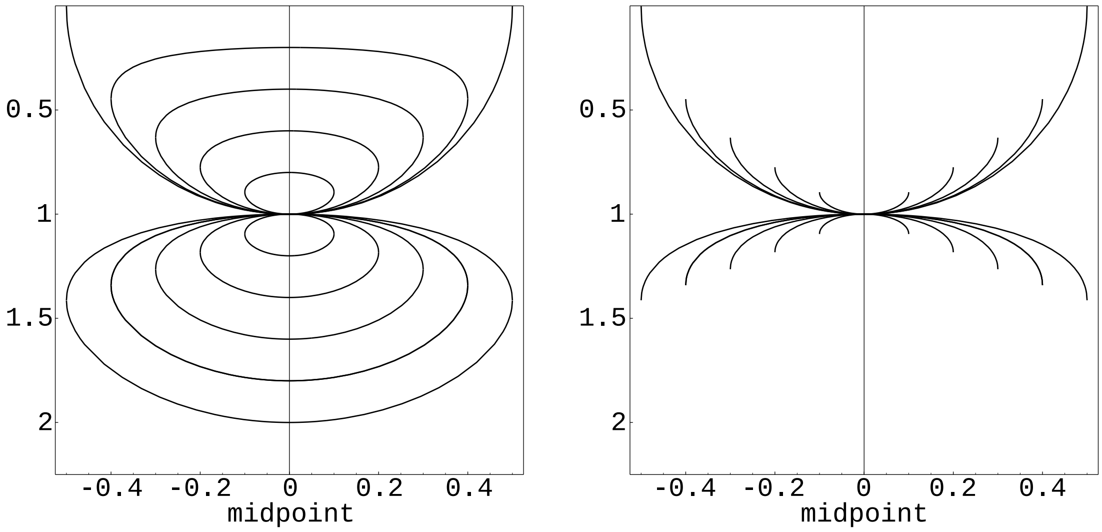

Figure 1.7: Constant-offset sections of the characteristic conoid - "offset continuation fronts" (left), and branches of the conoid used in the integral OC operator (right). The upper part of the plots (small times) corresponds to continuation to smaller offsets; the lower part (large times) corresponds to larger offsets. ofcon-con [CR]

As a second-order differential equation of the hyperbolic type, equation (1.1) describes two different processes. The first process is "forward" continuation from smaller to larger offsets, the second one is "reverse" continuation in the opposite direction. These two processes are clearly separated in the high-frequency asymptotics of operator (1.82). To obtain the asymptotical representation, it is sufficient to note that $\frac{1}{\sqrt{\pi}}\frac{H(t)}{\sqrt{t}}$ is the impulse response of the causal half-order integration operator and that $\frac{H(t^2-a^2)}{\sqrt{t^2-a^2}}$ is asymptotically equivalent to $\frac{H(t-a)}{\sqrt{2a}\sqrt{t-a}}$ $(t,a>0)$. Thus, the asymptotical form of the integral offset-continuation operator becomes

$$\begin{aligned} P^{(\pm)}(t_n,h,y) &= \mathbf{D}^{1/2}_{\pm t_n} \int w_0^{(\pm)}(\xi;h_1,h,t_n)\, P_1^{(0)}(\theta^{(\pm)}(\xi;h_1,h,t_n),y_1-\xi)\,d\xi \\ &\pm \mathbf{I}^{1/2}_{\pm t_n} \int w_1^{(\pm)}(\xi;h_1,h,t_n)\, P_1^{(1)}(\theta^{(\pm)}(\xi;h_1,h,t_n),y_1-\xi)\,d\xi\ . \end{aligned} \quad (1.87)$$

Here the signs "+" and "−" correspond to the type of continuation (the sign of $h-h_1$), $\mathbf{D}_{\pm t_n}^{1/2}$ and $\mathbf{I}_{\pm t_n}^{1/2}$ stand for the operators of causal and anticausal half-order differentiation and integration applied with respect to the time variable t_n, the summation paths $\theta^{(\pm)}(\xi;h_1,h,t_n)$ correspond to the two non-negative sections of the characteristic conoid (1.86) (Figure 1.7):

$$t_1 = \theta^{(\pm)}(\xi;h_1,h,t_n) = \frac{t_n}{h}\sqrt{\frac{U \pm V}{2}}\;, \tag{1.88}$$

where $U = h^2 + h_1^2 - \xi^2$, and $V = \sqrt{U^2 - 4h^2 h_1^2}$; ξ is the midpoint separation (the integration parameter), and $w_0^{(\pm)}$ and $w_1^{(\pm)}$ are the following weighting functions:

$$w_0^{(\pm)} = \frac{1}{\sqrt{2\pi}}\,\frac{\theta^{(\pm)}(\xi;h_1,h,t_n)}{\sqrt{t_n\,V}}\;, \tag{1.89}$$

$$w_1^{(\pm)} = \frac{1}{\sqrt{2\pi}}\,\frac{\sqrt{t_n}\,h_1}{\sqrt{V}\,\theta^{(\pm)}(\xi;h_1,h,t_n)}\;. \tag{1.90}$$

Expression (1.88) for the summation path of the OC operator was obtained previously by Stovas and Fomel (1993, 1996) and Biondi and Chemingui (1994a,b). A somewhat different form of it is proposed by Bagaini and Spagnolini (1996). I describe the kinematic interpretation of formula (1.88) in Appendix C.

In the high-frequency asymptotics, it is possible to replace the two terms in equation (1.87) with a single term (Fomel, 1996). The single-term expression is

$$P^{(\pm)}(t_n,h,y) = \mathbf{D}_{\pm t_n}^{1/2} \int w^{(\pm)}(\xi;h_1,h,t_n)\,P_1^{(0)}(\theta^{(\pm)}(\xi;h_1,h,t_n),y_1-\xi)\,d\xi\;, \tag{1.91}$$

where

$$w^{(+)} = \sqrt{\frac{\theta^{(+)}(\xi;h_1,h,t_n)}{2\pi}}\,\frac{h^2-h_1^2-\xi^2}{V^{3/2}}\;, \tag{1.92}$$

$$w^{(-)} = \frac{\theta^{(-)}(\xi;h_1,h,t_n)}{\sqrt{2\pi\,t_n}}\,\frac{h_1^2-h^2+\xi^2}{V^{3/2}}\;. \tag{1.93}$$

A more general approach to true-amplitude asymptotic offset continuation is developed by Santos et al. (1997).

The limit of expression (1.88) for the output offset h approaching zero can be evaluated by L'Hospitale's rule. As one would expect, it coincides with the well-known expression for the summation path of the integral DMO operator (Deregowski and Rocca, 1981)

$$t_1 = \theta^{(-)}(\xi; h_1, 0, t_n) = \lim_{h \to 0} \frac{t_n}{h} \sqrt{\frac{U-V}{2}} = \frac{t_n\, h_1}{\sqrt{h_1^2 - \xi^2}} \,. \tag{1.94}$$

I discuss the connection between offset continuation and DMO in the next section.

OFFSET CONTINUATION AND DMO

Dip moveout represents a particular case of offset continuation for the output offset equal to zero. In this section, I consider the DMO case separately in order to compare the solutions of equation (1.1) with the Fourier-domain DMO operators, which have been the standard for DMO processing since Hale's outstanding work (Hale, 1983, 1984).

Starting from equations (B.12)-(B.14) in Appendix B and setting the output offset to zero, we obtain the following DMO-like integral operators in the t–k domain:

$$\widetilde{P}(t_0, 0, k) = H(t_0) \left(\widetilde{P}_0(t_0, k) + t_0\, \widetilde{P}_1(t_0, k)\right) \,, \tag{1.95}$$

where

$$\widetilde{P}_0(t_0, k) = -\frac{\partial}{\partial t_0} \int_{t_0}^{\infty} \widetilde{P}_1^{(0)}(|t_1|, k)\; J_0\left(\frac{k\, h_1}{t_1} \sqrt{t_1^2 - t_0^2}\right) dt_1 \,, \tag{1.96}$$

$$\widetilde{P}_1(t_0, k) = -\int_{t_0}^{\infty} h_1\, \widetilde{P}_1^{(1)}(|t_1|, k)\; J_0\left(\frac{k\, h_1}{t_1} \sqrt{t_1^2 - t_0^2}\right) \frac{dt_1}{t_1^2} \,, \tag{1.97}$$

the wavenumber k corresponds to the midpoint axis y, and J_0 is the zeroth-order Bessel function. The Fourier transform of (1.96) and (1.97) with respect to the time variable t_0 reduces to known integrals (Gradshtein and Ryzhik, 1994) and creates explicit DMO-type operators in the frequency-wavenumber domain, as follows:

$$\widetilde{\widetilde{P}}_0(\omega_0,k) = i \int_{-\infty}^{\infty} \widetilde{P}_1^{(0)}(|t_1|,k)\, \frac{\sin(\omega_0\,|t_1|\,A)}{A}\, dt_1\;, \tag{1.98}$$

$$\widetilde{\widetilde{P}}_1(\omega_0,k) = i \int_{-\infty}^{\infty} h_1\, \widetilde{P}_1^{(1)}(|t_1|,k)\, \frac{\sin(\omega_0\,|t_1|\,A)}{A}\, \frac{dt_1}{t_1^2}\;, \tag{1.99}$$

where

$$A = \sqrt{1+\frac{(k\,h_1)^2}{(\omega_0\,t_1)^2}}\;, \tag{1.100}$$

$$\widetilde{\widetilde{P}}_j(\omega_0,k) = \int \widetilde{P}_j(t_0,k)\, \exp(i\,\omega_0 t_0)\, dt_0\;. \tag{1.101}$$

It is interesting to note that the first term of the continuation to zero offset (1.98) coincides exactly with the imaginary part of Hale's DMO operator (Hale, 1984). However, unlike Hale's, operator (1.95) is causal, which means that its impulse response does not continue to negative times. The non-causality of Hale's DMO and related issues are discussed in more detail by Stovas and Fomel (1996) and Fomel (1995).

Though Hale's DMO is known to provide correct reconstruction of the geometry of zero-offset reflections, it does not account properly for the amplitude changes (Black et al., 1993). The preceding section of this chapter shows that the additional contribution to the amplitude is contained in the second term of the OC operator (1.82), which transforms to the second term in the DMO operator (1.95). Note that this term vanishes at the input offset equal to zero, which represents the case of the inverse DMO operator.

Considering the inverse DMO operator as the continuation from zero offset to a non-zero offset, we can obtain its representation in the t-k domain from equations (B.12)-(B.14) as

$$\widetilde{P}(t_n,h,k) = H(t_n)\frac{\partial}{\partial t_n}\int_0^{t_n} \widetilde{P}_0(|t_0|,k)\; J_0\left(\frac{k\,h}{t_n}\sqrt{t_n^2-t_0^2}\right) dt_0\;, \tag{1.102}$$

Fourier transforming equation (1.102) with respect to the time variable t_0 according to equation (1.101), we get the Fourier-domain version of the "amplitude-preserving" inverse DMO:

$$\widetilde{P}(t_n,h,k) = \frac{H(t_n)}{2\pi}\,\frac{\partial}{\partial t_n}\int_{-\infty}^{\infty} \widetilde{\widetilde{P}}_0(\omega_0,k)\,\frac{\sin\left(\omega_0\,|t_n|\,A\right)}{\omega_0\,A}\,d\omega_0\;, \tag{1.103}$$

$$A = \sqrt{1+\frac{(k\,h)^2}{(\omega_0\,t_n)^2}}\;. \tag{1.104}$$

Comparing operator (1.103) with Ronen's version of inverse DMO (Ronen, 1987), one can see that if Hale's DMO is denoted by $\mathbf{D}_{t_0}\,\mathbf{H}$, then Ronen's inverse DMO is $\mathbf{H^T}\,\mathbf{D}_{-t_0}$, while the amplitude-preserving inverse (1.103) is $\mathbf{D}_{t_n}\,\mathbf{H^T}$. Here $\mathbf{D}_t$ is the derivative operator $\left(\frac{\partial}{\partial t}\right)$, and $\mathbf{H^T}$ stands for the adjoint operator defined by the dot-product test

$$(\mathbf{Hm},\mathbf{d}) = (\mathbf{m},\mathbf{H^T d}), \tag{1.105}$$

where the parentheses denote the dot product:

$$(\mathbf{m_1},\mathbf{m_2}) = \int\int m_1(t_n,y)\,m_2(t_n,y)\,dt_n\,dy\;.$$

In high-frequency asymptotics, the difference between the amplitudes of the two inverses is simply the Jacobian term $\frac{dt_0}{dt_n}$, asymptotically equal to $\frac{t_0}{t_n}$. This difference corresponds exactly to the difference between Black's definition of amplitude preservation (Black et al., 1993) and the definition used in Born DMO (Bleistein, 1990; Liner, 1991), as discussed above. While operator (1.103) preserves amplitudes in the Born DMO sense, Ronen's inverse satisfies Black's amplitude preservation criteria. This means Ronen's operator implies that the "geometric spreading" correction (multiplication by time) has been performed on the data prior to DMO.

To construct a one-term DMO operator, thus avoiding the estimation of the offset derivative in (1.90), let us consider the problem of inverting the inverse DMO operator (1.103). One of the possible approaches to this problem is the least-squares iterative inversion, as proposed by Ronen (1987). This requires constructing the adjoint operator, which is Hale's DMO (or its analog) in the case of Ronen's method. The iterative least-squares approach can account for irregularities in the data geometry (Ronen et al., 1991; Ronen, 1994) and boundary effects, but it is computationally expensive because of the multiple application of the operators. An alternative approach is the asymptotic inversion, which can be viewed as a special case of preconditioning the adjoint operator (Liner and Cohen, 1988; Chemingui and Biondi, 1996). The goal of the asymptotical inverse is to reconstruct the geometry and the amplitudes of the reflection events in the high-frequency asymptotical limit.

According to Beylkin's theory of asymptotical inversion, also known as the *generalized Radon transform* (Beylkin, 1985), two operators of the form

$$D(\omega) = \int X(t,\omega)\, M(t)\, \exp\left[i\,\omega\phi(t,\omega)\right] dt \tag{1.106}$$

and

$$\widetilde{M}(t) = \int Y(t,\omega)\, D(\omega)\, \exp\left[-i\,\omega\phi(t,\omega)\right] d\omega \tag{1.107}$$

constitute a pair of asymptotically inverse operators ($\widetilde{M}(t)$ matching $M(t)$ in the high-frequency asymptotics) if

$$X(t,\omega)\,Y(t,\omega) = \frac{Z(t,\omega)}{2\pi}\,, \tag{1.108}$$

where Z is the “Beylkin determinant”

$$Z(t,\omega) = \left|\frac{\partial \omega}{\partial \hat{\omega}}\right| \text{ for } \hat{\omega} = \omega\,\frac{\partial \phi(t,\omega)}{\partial t}\,. \tag{1.109}$$

With respect to the high-frequency asymptotical representation, we can recast (1.103) in the equivalent form by moving the time derivative under the integral sign:

$$\widetilde{P}(t_n,k) \approx \frac{H(t_n)}{2\pi}\,\mathrm{Re}\left[\int_{-\infty}^{\infty} A^{-2}\,\widetilde{\widetilde{P}}_0(\omega_0,k)\,\exp(-i\omega_0\,|t_n|\,A)\,d\omega_0\right] \tag{1.110}$$

Now the asymptotical inverse of (1.110) is evaluated by means of Beylkin's method (1.106)-(1.107), which leads to an amplitude-preserving one-term DMO operator of the form

$$\widetilde{\widetilde{P}}_0(\omega_0,k) = \mathrm{Im}\left[\int_{-\infty}^{\infty} B\,\widetilde{P}_1^{(0)}(|t_1|,k)\,\exp(i\omega_0\,|t_1|\,A)\,dt_1\right]\,, \tag{1.111}$$

where

$$B = A^2\,\frac{\partial}{\partial \omega_0}\left(\omega_0\,\frac{\partial(t_n\,A)}{\partial t_n}\right) = A^{-1}\,(2\,A^2-1)\,. \tag{1.112}$$

The amplitude factor (1.112) corresponds exactly to that of Born DMO (Bleistein, 1990) in full accordance with the conclusions of the asymptotical analysis of the offset-continuation amplitudes. An analogous result can be obtained with the different definition of amplitude preservation proposed by Black et al. (1993). In the time-and-space domain, the operator asymptotically analogous to (1.111) is found by applying either the stationary phase technique (Liner, 1990; Black et al., 1993) or Goldin's method of discontinuities (Goldin, 1988, 1990), which is the time-and-space analog of Beylkin's asymptotical inverse theory (Stovas and Fomel, 1996). The time-and-space asymptotical DMO operator takes the form

$$P_0(t_0,y) = \mathbf{D}_{-t_0}^{1/2} \int w_0(\xi;h_1,t_0)\, P_1^{(0)}(\theta^{(-)}(\xi;h_1,0,t_0), y_1-\xi)\, d\xi \;, \tag{1.113}$$

where the weighting function w_0 is defined as

$$w_0(\xi;h_1,t_0) = \sqrt{\frac{t_0}{2\pi}}\, \frac{h_1\,(h_1^2+\xi^2)}{(h_1^2-\xi^2)^2} \;. \tag{1.114}$$

OFFSET CONTINUATION IN THE LOG-STRETCH DOMAIN

The log-stretch transform, proposed by Bolondi et al. (1982) and further developed by many other researchers, has proven a useful tool in DMO and OC processing. Applying a log-stretch transform of the form

$$\sigma = \ln\left|\frac{t_n}{t_*}\right| \;, \tag{1.115}$$

where t_* is an arbitrarily chosen time constant, eliminates the time dependence of the coefficients in equation (1.1) and therefore makes this equation invariant to time shifts. After the double Fourier transform with respect to the midpoint coordinate y and to the transformed (log-stretched) time coordinate σ, the partial differential equation (1.1) takes the form of an ordinary differential equation,

$$h\left(\frac{d^2\widehat{\widehat{P}}}{dh^2} + k^2\,\widehat{\widehat{P}}\right) = i\Omega\,\frac{d\widehat{\widehat{P}}}{dh} \;, \tag{1.116}$$

where

$$\widehat{\widehat{P}}(h) = \int\!\!\int P(t_n = t_*\,\exp(\sigma), h, y)\,\exp(i\Omega\sigma - iky)\,d\sigma\,dy \;. \tag{1.117}$$

Equation (1.116) has the known general solution, expressed in terms of cylinder functions of complex order $\lambda = \frac{1+i\Omega}{2}$ (Watson, 1952)

$$\widehat{\widehat{P}}(h) = C_1(\lambda)\,(kh)^{\lambda}\,J_{-\lambda}(kh) + C_2(\lambda)\,(kh)^{\lambda}\,J_{\lambda}(kh)\,, \tag{1.118}$$

where $J_{-\lambda}$ and J_{λ} are Bessel functions, and C_1 and C_2 stand for some arbitrary functions of λ that do not depend on k and h.

In the general case of offset continuation, C_1 and C_2 are constrained by the two initial conditions (1.80) and (1.81). In the special case of continuation from zero offset, we can neglect the second term in (1.118) as vanishing at the zero offset. The remaining term defines the following operator of inverse DMO in the Ω, k domain:

$$\widehat{\widehat{P}}(h) = \widehat{\widehat{P}}(0)\,Z_{\lambda}(kh)\,, \tag{1.119}$$

where Z_{λ} is the analytic function

$$\begin{aligned} Z_{\lambda}(x) &= \Gamma(1-\lambda)\left(\frac{x}{2}\right)^{\lambda} J_{-\lambda}(x) = {}_0F_1\left(;1-\lambda;-\frac{x^2}{4}\right) \\ &= \sum_{n=0}^{\infty} \frac{(-1)^n}{n!}\,\frac{\Gamma(1-\lambda)}{\Gamma(n+1-\lambda)}\left(\frac{x}{2}\right)^{2n}\,, \end{aligned} \tag{1.120}$$

Γ is the gamma function and ${}_0F_1$ is the confluent hypergeometric limit function (Petkovsek et al., 1996).

The DMO operator now can be derived as the inversion of operator (1.119), which is a simple multiplication by $1/Z_{\lambda}(kh)$. Therefore, offset continuation becomes a multiplication by $Z_{\lambda}(kh_2)/Z_{\lambda}(kh_1)$ (the cascade of two operators). This fact demonstrates an important advantage of moving to the log-stretch domain: both offset continuation and DMO are simple filter multiplications in the Fourier domain of the log-stretched time coordinate.

In order to compare operator (1.119) with the known versions of log-stretch DMO, we need to derive its asymptotical representation for high frequency Ω. The required asymptotic expression follows directly from the definition of function Z_{λ} in (1.120) and the known asymptotical representation for a Bessel function of high order (Watson, 1952):

$$J_\lambda(\lambda z) \overset{\lambda\to\infty}{\approx} \frac{(\lambda z)^\lambda \exp\left(\lambda\sqrt{1-z^2}\right)}{e^\lambda\,\Gamma(\lambda+1)\,(1-z^2)^{1/4}\left\{1+\sqrt{1-z^2}\right\}^{\sqrt{1-z^2}}}\,. \tag{1.121}$$

Substituting approximation (1.121) into (1.120) and considering the high-frequency limit of the resultant expression yields

$$Z_\lambda(kh) \approx \left\{\frac{1+\sqrt{1-\left(\frac{kh}{\lambda}\right)^2}}{2}\right\}^\lambda \frac{\exp\left(\lambda\left[1-\sqrt{1-\left(\frac{kh}{\lambda}\right)^2}\right]\right)}{\left(1-\left(\frac{kh}{\lambda}\right)^2\right)^{1/4}} \approx F(\epsilon)\,e^{i\Omega\,\psi(\epsilon)}\,, \tag{1.122}$$

where ϵ denotes the ratio $\frac{2kh}{\Omega}$,

$$F(\epsilon) = \sqrt{\frac{1+\sqrt{1+\epsilon^2}}{2\sqrt{1+\epsilon^2}}}\,\exp\left(\frac{1-\sqrt{1+\epsilon^2}}{2}\right)\,, \tag{1.123}$$

and

$$\psi(\epsilon) = \frac{1}{2}\left(1-\sqrt{1+\epsilon^2}+\ln\left(\frac{1+\sqrt{1+\epsilon^2}}{2}\right)\right)\,. \tag{1.124}$$

Asymptotical representation (1.122) is valid for high frequency Ω and $|\epsilon| \leq 1$. It can be shown that the phase function ψ defined in (1.124) coincides precisely with the analogous term in Liner's *exact log DMO* (Liner, 1990), which was proven to provide the correct geometric properties of DMO. Similar expressions for the log-stretch phase factor ψ were derived in different ways by Zhou et al. (1996) and Canning and Gardner (1996). However, the amplitude term $F(\epsilon)$ differs from the previously published ones because of the difference in the amplitude preservation properties.

A number of approximate log DMO operators have been proposed in the literature. As shown by Liner (1990), all of them but exact log DMO distort the geometry of reflection effects at large offsets. The distortion is caused by the implied approximations of the true phase function ψ. Bolondi's OC operator (Bolondi et al., 1982) implies $\psi(\epsilon) \approx -\frac{\epsilon^2}{8}$, Notfors' DMO (Notfors and Godfrey, 1987) implies $\psi(\epsilon) \approx 1 - \sqrt{1+(\epsilon/2)^2}$, and the "full DMO" (Bale and Jakubowicz, 1987) has $\psi(\epsilon) \approx \frac{1}{2}\ln\left[1-(\epsilon/2)^2\right]$. All these approximations are valid for small ϵ (small offsets or small reflector dips) and have errors of the order of ϵ^4 (Figure 1.8). The range of validity of Bolondi's operator is defined in equation (1.22).

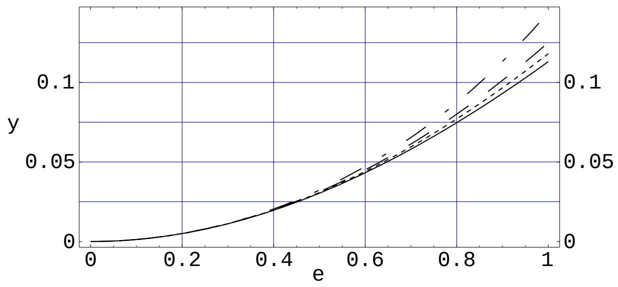

Figure 1.8: Phase functions of the log DMO operators. Solid line: exact log DMO; dashed line: Bolondi's OC; dashed-dotted line: Bale's full DMO; dotted line: Notfors' DMO. ofcon-pha [CR]

In practice, seismic data are often irregularly sampled in space but regularly sampled in time. This makes it attractive to apply offset continuation and DMO operators in the $\{\Omega, y\}$ domain, where the frequency Ω corresponds to the log-stretched time and y is the midpoint coordinate. Performing the inverse Fourier transform on the spatial frequency transforms the inverse DMO operator (1.119) to the $\{\Omega, y\}$ domain, where the filter multiplication becomes a convolutional operator:

$$\widehat{P}(\Omega,h,y) = \frac{\widehat{F}(\Omega)}{\sqrt{2\pi}} \int_{|\xi|<h} \frac{h}{h^2-\xi^2}\,\widehat{P}_0(\Omega,y-\xi)\,\exp\left(-\frac{i\Omega}{2}\ln\left(1-\frac{\xi^2}{h_1^2}\right)\right)d\xi\ . \qquad (1.125)$$

Here $\widehat{F}(\Omega)$ is a high-pass frequency filter:

$$\widehat{F}(\Omega) = \frac{\Gamma(1/2 - i\Omega/2)}{\sqrt{1/2}\,\Gamma(-i\Omega/2)}\ . \qquad (1.126)$$

At high frequencies $\widehat{F}(\Omega)$ is approximately equal to $(-i\Omega)^{1/2}$, which corresponds to the half-derivative operator $\left(\frac{\partial}{\partial\sigma}\right)^{1/2}$, which, in turn, is equal to the $\left(t_n\frac{\partial}{\partial t_n}\right)^{1/2}$ term of the asymptotical OC operator (1.87). The difference between the exact filter $\widehat{F}$ and its approximation by the half-order derivative operator is shown in Figure 1.9. This difference is a measure of the validity of asymptotical OC operators.

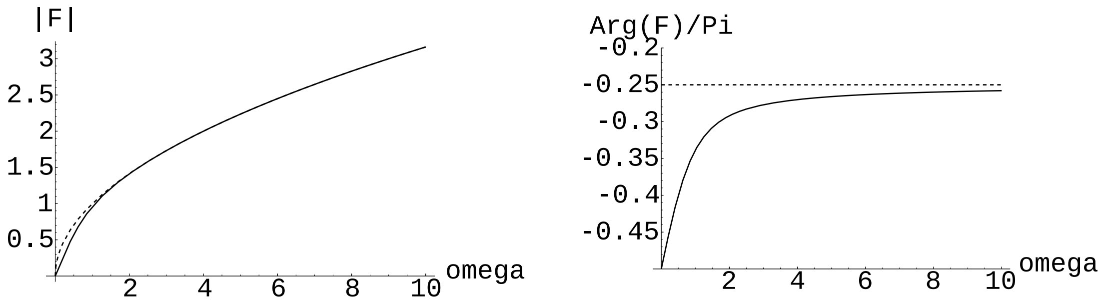

Figure 1.9: Amplitude (left) and phase (right) of the time filter in the log-stretch domain. The solid line is for the exact filter; the dashed line for its approximation by the half-order derivative filter. ofcon-flt [CR]

Inverting operator (1.125), we can obtain the DMO operator in the $\{\Omega, y\}$ domain.

DISCUSSION

The differential model for offset continuation is based on several assumptions. It is important to fully realize them in order to understand the practical limitations of this model.

- The *constant velocity* assumption is essential for theoretical derivations. In practice, this limitation is not too critical, because the effects of velocity heterogeneity are partially compensated by the normal moveout correction. DMO and offset continuation algorithms based on the constant-velocity assumptions are widely used in practice (Hale, 1995).

- The *single-mode* assumption does not include multiple reflections in the model. If multiple events (with different apparent velocities) are present in the data, they might require extending the model. Convolving two (or more) differential offset continuation operators, corresponding to different velocities, we can obtain a higher-order differential operator for predicting multiple events.

- The *continuous AVO* assumption implies that the reflectivity variation with offset is continuous and can be neglected in a local neighborhood of a particular offset. While the offset continuation model correctly predicts the geometric spreading effects in the reflected wave amplitudes, it does not account for the variation of the reflection coefficient with offset.

- The *2.5-D* assumption was implicit in the derivation of the offset continuation equation. According to this assumption, the reflector does not change in the cross-line direction, and we can always consider the reflection plane in two dimensions. We can remove the 2.5-D assumption by considering a system of two offset continuation equations, acting in two orthogonal directions. The first equation would involve in-line midpoint and in-line offset, and the second equation would involve cross-line midpoint and cross-line offset.

CONCLUSIONS

I have introduced a partial differential equation (1.1) and proved that the process described by it provides for a kinematically and dynamically equivalent offset continuation transform. Kinematic equivalence means that in constant velocity media the reflection traveltimes are transformed to their true locations on different offsets. Dynamic equivalence means that, in the OC process, the geometric spreading term in the amplitudes of reflected waves transforms in accordance with the geometric seismics laws, while the angle-dependent reflection coefficient stays the same.

The offset continuation equation can be applied directly to design OC operators of the finite-difference type. To construct integral OC operators, I have posed and solved an initial value problem for the offset continuation equation (1.1). For the special cases of continuation to zero offset (DMO) and continuation from zero offset (inverse DMO), the OC operators are related to the known forms of DMO operators: Hale's Fourier DMO, Born DMO, and Liner's "exact log DMO." The discovery of these relations sheds additional light on the problem of amplitude preservation in DMO.

ACKNOWLEDGMENTS

Sergey Goldin drew my attention to the role of curvature dependence in reflected wave amplitudes (Goldin and Fomel, 1995). I also acknowledge the support of Alexey Stovas, who introduced me to the world of DMO and collaborated with me on developing the asymptotic theory of offset continuation (Stovas and Fomel, 1996). Norm Bleistein suggested the Kirchhoff modeling test and collaborated with me on carrying it out (Fomel and Bleistein, 1996; Fomel et al., 1996). Shuki Ronen and Richard Bale pointed out to me the importance of the log-stretch domain in DMO and related problems. I appreciate the encouragement of Fabio Rocca regarding the analysis of the offset-continuation partial differential equation.

Bibliography

Babich, V. M., 1991, Short-wavelength diffraction theory: asymptotic methods: Springer-Verlag, Berlin; New York.

Bagaini, C., and Spagnolini, U., 1993, Common shot velocity analysis by shot continuation operator: 63rd Annual Internat. Mtg., Soc. Expl. Geophys., Expanded Abstracts, 673–676.

Bagaini, C., and Spagnolini, U., 1996, 2-D continuation operators and their applications: Geophysics, **61**, no. 06, 1846–1858.

Bagaini, C., Spagnolini, U., and Pazienza, V. P., 1994, Velocity analysis and missing offset restoration by prestack continuation operators: 64th Annual Internat. Mtg., Soc. Expl. Geophys., Expanded Abstracts, 1549–1552.

Bale, R., and Jakubowicz, H., 1987, Post-stack prestack migration: 57th Annual Internat. Mtg., Soc. Expl. Geophys., Expanded Abstracts, Session:S14.1.

Beylkin, G., 1985, Imaging of discontinuities in the inverse scattering problem by inversion of a causal generalized Radon transform: Journal of Mathematical Physics, **26**, 99–108.

Biondi, B., and Chemingui, N., 1994a, Transformation of 3-D prestack data by Azimuth Moveout: SEP–**80**, 125–143.

Biondi, B., and Chemingui, N., 1994b, Transformation of 3-D prestack data by azimuth moveout (AMO): 64th Ann. Internat. Mtg., Soc. Expl. Geophys., Expanded Abstracts, 1541–1544.

Biondi, B., Fomel, S., and Chemingui, N., 1998, Azimuth moveout for 3-D prestack imaging: Geophysics, **63**, no. 02, 574–588.

Black, J. L., Schleicher, K. L., and Zhang, L., 1993, True-amplitude imaging and dip moveout: Geophysics, **58**, no. 1, 47–66.

Bleistein, N., and Cohen, J. K., 1995, The effect of curvature on true amplitude DMO: Proof of concept: ACTI, 4731U0015-2F; CWP-193, Colorado School of Mines.

Bleistein, N., 1984, Mathematical methods for wave phenomena: Academic Press Inc. (Harcourt Brace Jovanovich Publishers), New York.

Bleistein, N., 1990, Born DMO revisited: 60th Annual Internat. Mtg., Soc. Expl. Geophys., Expanded Abstracts, 1366–1369.

Bolondi, G., Loinger, E., and Rocca, F., 1982, Offset continuation of seismic sections: Geophys. Prosp., **30**, no. 6, 813–828.

Canning, A., and Gardner, G. H. F., 1996, Regularizing 3-D data sets with DMO: Geophysics, **61**, no. 04, 1103–1114.

Chemingui, N., and Biondi, B., 1996, Handling the irregular geometry in wide azimuth surveys: 66th Annual Internat. Mtg., Soc. Expl. Geophys., Expanded Abstracts, 32–35.

Claerbout, J. F., 1976, Fundamentals of geophysical data processing: Blackwell.

Courant, R., 1962, Methods of mathematical physics: Interscience Publishers, New York.

Deregowski, S. M., and Rocca, F., 1981, Geometrical optics and wave theory of constant offset sections in layered media: Geophys. Prosp., **29**, no. 3, 374–406.

Fomel, S., and Biondi, B., 1995, The time and space formulation of azimuth moveout: 65th Ann. Internat. Mtg., Soc. Expl. Geophys., Expanded Abstracts, 1449–1452.

Fomel, S., and Bleistein, N., 1996, Amplitude preservation for offset continuation: Confirmation for Kirchhoff data: SEP–**92**, 219–227.

Fomel, S., Bleistein, N., Jaramillo, H., and Cohen, J. K., 1996, True amplitude DMO, offset continuation and AVA/AVO for curved reflectors: 66th Annual Internat. Mtg., Soc. Expl. Geophys., Expanded Abstracts, 1731–1734.

Fomel, S. B., 1994, Kinematically equivalent differential operator for offset continuation of seismic sections: Russian Geology and Geophysics, **35**, no. 9, 122–134.

Fomel, S., 1995, Amplitude preserving offset continuation in theory Part 2: Solving the equation: SEP–**89**, 109–132.

Fomel, S., 1996, Stacking operators: Adjoint versus asymptotic inverse: SEP–**92**, 267–292.

Gazdag, J., 1978, Wave equation migration with the phase shift method: Geophysics, **43**, 1342–1351.

Goldin, S. V., and Fomel, S. B., 1995, Estimation of reflection coefficient in DMO: Russian Geology and Geophysics, **36**, no. 4, 103–115.

Goldin, S. V., 1988, Transformation and recovery of discontinuities in problems of tomographic type: Institute of Geology and Geophysics, Novosibirsk (in Russian).

Goldin, S., 1990, A geometric approach to seismic processing: the method of discontinuities: SEP–**67**, 171–210.

Goldin, S. V., 1994, Superposition and continuation of tranformations used in seismic migration: Russian Geology and Geophysics, **35**, no. 9, 131–145.

Gradshtein, I. S., and Ryzhik, I. M., 1994, Table of integrals, series, and products: Boston: Academic Press.

Haddon, R. A. W., and Buchen, P. W., 1981, Use of Kirchhoff's formula for body wave calculations in the earth: Geophys. J. Roy. Astr. Soc., **67**, 587–598.

Hale, I. D., 1983, Dip moveout by Fourier transform: Ph.D. thesis, Stanford University.

Hale, D., 1984, Dip-moveout by Fourier transform: Geophysics, **49**, no. 6, 741–757.

Hale, D., 1991, Course notes: Dip moveout processing: Soc. Expl. Geophys.

Hale, D., Ed. **DMO processing**. Society Of Exploration Geophysicists, 1995.

Liner, C. L., and Cohen, J. K., 1988, An amplitude-preserving inverse of Hale‘s DMO: 58th Annual Internat. Mtg., Soc. Expl. Geophys., Expanded Abstracts, 1117–1120.

Liner, C., 1990, General theory and comparative anatomy of dip moveout: Geophysics, **55**, no. 5, 595–607.

Liner, C. L., 1991, Born theory of wave-equation dip moveout: Geophysics, **56**, no. 2, 182–189.

Notfors, C. D., and Godfrey, R. J., 1987, Dip moveout in the frequency-wavenumber domain (short note): Geophysics, **52**, no. 12, 1718–1721.

Petkovsek, M., Wilf, H. S., and Zeilberger, D., 1996, $A = B$: A K Peters Ltd., Wellesley, MA.

Ronen, S., Sorin, V., and Bale, R., 1991, Spatial dealiasing of 3-D seismic reflection data: Geophysical Journal International, pages 503–511.

Ronen, J., 1987, Wave equation trace interpolation: Geophysics, **52**, no. 7, 973–984.

Ronen, S., 1994, Handling irregular geometry: Equalized DMO and beyond: 64th Ann. Internat. Mtg., Soc. Expl. Geophys., Expanded Abstracts, 1545–1548.

Santos, L. T., Schleicher, J., and Tygel, M., 1997, 2.5-D true-amplitude offset continuation: Journal of Seismic Exploration, **6**, no. 2-3, 103–116.

Schwab, M., 1993, Shot gather continuation: SEP–**77**, 117–130.

Stolt, R. H., 1978, Migration by Fourier transform: Geophysics, **43**, no. 1, 23–48.

Stovas, A. M., and Fomel, S. B., 1993, Kinematically equivalent DMO operators: Presented at the SEG-Moscow, SEG-Moscow.

Stovas, A. M., and Fomel, S. B., 1996, Kinematically equivalent integral DMO operators: Russian Geology and Geophysics, **37**, no. 2, 102–113.

Tenenbaum, M., and Pollard, H., 1985, Ordinary differential equations : an elementary textbook for students of mathematics, engineering, and the sciences: Dover Publications.

Červený, V., Molotkov, I. A., and Pšenčik, I., 1977, Ray method in seismology: Univerzita Karlova, Praha.

Watson, G. N., 1952, A treatise on the theory of Bessel functions: Cambridge University Press, 2nd edition.

Zhou, B., Mason, I. M., and Greenhalgh, S. A., 1996, An accurate formulation of log-stretch dip moveout in the frequency-wavenumber domain: Geophysics, **61**, no. 03, 815–820.